СООБЩЕНИЯ
ОБЪЕДИНЕННОГО
ИНСТИТУТА
ЯДЕРНЫХ
ИССЛЕДОВАНИЙ

Дубна

E1-97-214

DELTA ISOBAR PRODUCTION IN THE $^4He p \to {}^3H p n \pi^+$ REACTION

1997

1 Introduction

In the interactions of the lightest nuclei with protons the mechanism of collective $\Delta(1232)$ isobar excitation is suppressed. This mechanism manifests itself with greater widths of the peak and shifts to smaller excitation energies as well as with an increase of the cross section per nucleon compared to the quasi-free isobar excitations [1, 2] and other references therein. Mainly just the latter take place in the light nuclei-proton interactions. This has been shown in our previous work [3], where the $dp \to p\pi^+X$ reaction at 3.34 GeV/c of the incoming deuteron momenta has been studied. As one can see in Fig. 1 the invariant masses displayed on the scatter plot $(M_X, M_{p\pi})$ split up. Assuming a spectator neutron from the incoming deuteron, the observed mass splitting could have been described by a quasi-free proton - proton reaction

$$p_d p_t \to pn\pi^+, \tag{1}$$

where p_t and p_d denote the target and projectile protons, respectively, and p and π^+ come from the $\Delta^{++}(1232)$ isobar decay. The events tend to form two groups: in one of them the Δ^{++} can be related to the excited free target proton p_t, while in the other the quasi-free proton of the deuteron does the same. The two pronounced maxima present in the momentum distribution of the $(p\pi^+)$ system (Fig. 2) also support the identification of two groups of events with different vertices. Fast combinations in this frame are connected with the impinging proton while the slow ones with the nucleon from the nucleus. Our previous papers [4] on light nuclei fragmentation have demonstrated that the nuclear fragments in most cases do not participate in the interaction, i.e. they are spectators. So, by analogy with (1) it is reasonable to

study the reaction

$$^4Hep \rightarrow {}^3H_s pn\pi^+ \tag{2}$$

(^3H_s being a spectator) and to expect a quasi-free p-p interaction of the form:

$$p_{^4He}p_t \rightarrow pn\pi^+, \tag{3}$$

with $p_{^4He}$ and p_t being the projectile and target protons, respectively.

2 Experiment

The experimental data have been obtained using the JINR LHE 1m hydrogen bubble chamber irradiated with ^4He beam of 8.6 GeV/c. The number of events in different reaction channels and corresponding cross sections can be found in [5]. To select the desired subsample (2) of the $^4Hep \rightarrow {}^3Hpn\pi^+$ reaction, enriched with events containing a triton spectator, the analysis is constrained to the events in which ^3H is the slowest particle in the ^4He nucleus rest frame. Such a selection results in 2,581 events with the corresponding cross section $\sigma = (9.7 \pm 0.2)mb$. The momentum distribution of the tritons is of a typical spectator-like shape (with an average $< p >= 187MeV/c$) and with production angle cosine distributed uniformly. Because in this energy region pions are produced predominantly via Δ isobar and its consecutive decay to pion and nucleon, one can assume that the reaction (3) mainly proceeds as

$$p_{^4He}p_t \rightarrow \Delta^{++}n,\ \Delta^{++} \rightarrow p\pi^+ \tag{4}$$

or

$$p_{^4He}p_t \rightarrow \Delta^+p,\ \Delta^+ \rightarrow n\pi^+, \tag{5}$$

where the cross section for (5) is about 6 times smaller than for (4) [6].

3 Discussion

The invariant mass plot $M(^3H_sn)$ versus $M(p\pi^+)$ is shown in Fig. 3. It can be seen that the experimental values are not distributed uniformly, they group into two areas: the lower $M(^3H_sn) \in (3.76, 3.90)\ GeV/c^2$ and the upper $M(^3H_sn) \in (4.34, 4.48)\ GeV/c^2$ ones, while the values of $M(p\pi^+)$ are practically the same, being in both cases $M(p\pi^+) \in (1.18, 1.24)\ GeV/c^2$ (close to the mass of the Δ isobar). This splitting can be understood by analogy with [3] from the kinematical analysis of the reaction (4).

Possible diagrams of isobar production in the reaction (4) are displayed in Fig. 4, (a,c) one-pion exchange and (b,d) momentum diagrams in the CMS. It can be written:

$$M^2(^3H_sn) = M_n^2 + M_{^3H_s}^2 + 2E_n^*E_{^3H_s}^* - 2p_n^*p_{^3H_s}^*\cos\theta^*, \tag{6}$$

where M_n and $M_{^3H_s}$ are the neutron and triton masses, $E_n^*, E_{^3H_s}^*$ and $p_n^*, p_{^3H_s}^*$ their CMS energies and momenta, respectively and θ^* is the angle between the momenta (proton off-mass shell effects in ^4He are neglected). The neutron energy E_n^* and momentum p_n^* are determined with the mass of the associately produced Δ^{++} isobar in (4). For the angle θ^* the following relations hold: $0 \leq \theta^* \leq \pi/2$ in the case of the target proton p_t excitation (proton vertices in Fig. 4a,b) and $\pi/2 \leq \theta^* \leq \pi$ for the projectile proton $p_{^4He}$ excitation (helium vertices in Fig. 4c,d). The limiting curve equations in the $(M_{^3H_sn}, M_{p\pi})$ plane can be obtained by setting $\theta^* = 0$ for the proton and $\theta^* = \pi$ for the helium vertices:

$$M_{^3H_sn}^2(p) = M_n^2 + M_{^3H_s}^2 + 2E_n^*E_{^3H_s}^* \pm 2p_n^*p_{^3H_s}^*, \tag{7}$$

where the sign '-' corresponds to the proton vertex, '+' is for the helium one. The equation of the curve, separating the events from different vertices is determined by the condition $\theta^*_n = \theta^* = \pi/2$:

$$M^2_{^3H,n}(0) = M^2_n + M^2_{^3H} + 2E^*_n E^*_{^3H}. \quad (8)$$

The Δ production cross section decreases with increasing |t| (t being the four-momentum transfer squared from the impinging proton to the fastest nucleon) and increasing of the Δ production angle [1]. It means that an abundant anisotropy appears in the production angle of neutrons (isobars) in the centre of mass system of the scattering protons. Therefore in the case of the free proton excitation (proton vertices) the angle θ^* is around 0 and θ^* is near to π for the proton from the nucleus (helium vertices). So, the events corresponding to isobar production then will mainly lay on the $(M_{^3H,n}, M_{p\pi})$ plot near the limiting curve as it can be seen in Fig. 3. The Fermi motion of the proton, neglected in the calculation of the boundary lines, can lead to some smearing of the experimental values. One can obtain the same results selecting events according to the leading proton (Fig. 4 a) and neutron (Fig. 4 c) in nucleus rest frame.

The splitting into two groups can also be supported by the two pronounced maxima in the $p\pi^+$ pair momentum distribution with respect to the helium rest frame (Fig. 5). The same tendency is observed as for the dp interaction (Fig. 2). While the splitting of events into upper and lower groups in Fig.3 can be explained by the anisotropical angular distribution of the neutrons from quasi nucleon - nucleon $pp \rightarrow p\pi^+ n$ scattering [7], the difference in their populations may be ascribed to the asymetry of the mentioned angular distribution. The value of the neutron backward

to forward ratio in quasi pp CMS is 1.43 ± 0.04, which corresponds, within the errors, to the ratio of the events in 'proton' and 'nuclear' vertices 1.54 ± 0.04. The smaller difference in populations of the analogous groups from $dp \rightarrow p\pi^+ X$ (nofit) [3] reactions, is connected with an admixture of spectator protons into $(p\pi^+)$ combinations, which is difficult to get rid of applying only a cut to proton momentum. In Fig. 6 the bump at greater values of the missing mass decreases with increasing cuts applied to the proton momentum, i.e. the number of events in the 'nuclear' vertex lessens.

The Dalitz plot ($(n\pi^+)$ - invariant mass squared versus $(p\pi^+)$ - invariant mass squared) presented in Fig. 7 shows that the experimental values are concentrated in a vertical zone in the $M^2_{p\pi^+}$ area corresponding to the Δ^{++} isobar mass.

The invariant mass M_Δ distribution for Δ production in free particle interactions is well described by the model with an energy depending isobar width [8]. In the quasi - free interaction is the situation more complex because of the Fermi - motion.

The $(p\pi^+)$ invariant mass distributions for the proton and helium vertices together with the results computed according to the Jackson formula [8] are displayed in Fig. 8. The limits of these distributions are: $M_{p\pi}$ (min) $= m_p + m_\pi$ and $M_{p\pi}$(max) $= \sqrt{s} - m_n$ ($\sqrt{s}$ is the CMS reaction energy of $p_{^4He} + p_t \rightarrow \Delta^{++} + n$), the $M_{p\pi}(max)$ value for the model distribution is equal 1543 MeV/c^2 (for momentum of proton from ^4He being 2.15 GeV/c). The mean values similarly as in [3] are shifted to greater masses compared to the computed ones. While the agreement between the experimental and computed distributions is acceptable at the lower masses, there is a disagreement at the higher ones. Since the Jackson formula reproduces well the

isobar masses in the experiments with free protons [9, 10, 11], the deviations can be connected to the neglected Fermi motion. This additional momentum smears the $\sqrt{s}$ distribution leading to enhanced width. It can be seen from Table 1 (containing the computed and experimental values). Table 1 contains the results on $\Delta^{++}(1232)$ isobar production from the studied experiment as well as from other experiments. In the rows 1 and 3 there are computed results according to [8], values from this experiment are in the row 4, the row 2 contains the values from Δ^{++} production in $dp \rightarrow p\pi^+n$ reaction [3], row 5 the experimental values from $K^+p \rightarrow K^0\Delta^{++}$ reaction [9] and in rows 6,7 there are values from $pp \rightarrow \Delta^{++}n$ reaction [10, 11]. Experimental values in [3, 9, 10] have also been obtained by means of bubble chamber method, while the data in [11] are from magnetic spectrometer.

Conclusion

Similar features of the Δ^{++} production have been observed in the dp and ^4Hep interactions. The splitting of the $(p\pi^+)$ combinations into two groups is determined by kinematical effects in the quasi nucleon - nucleon reaction. The characteristics of the Δ^{++} isobar (mass, width and shape of the distribution) produced in different vertices are closed to each other and agree with other experimental results.

Acknowledgments

This work was partly supported by the Grant Agency for Science at the Ministry of Education of the Slovak Republic.

Table 1 Data on $\Delta^{++}(1232)$ isobar production. Rows 1 and 3 are computed results according to [8], the rest are experimental results. Results of the present work are without reference number. Notation: p means the incoming proton momenta, $M_\Delta(p)$, $\Gamma_\Delta(p)$ and $M_\Delta(A)$, $\Gamma_\Delta(A)$ are the masses, widths of the Δ isobar produced in the proton and nuclear vertices, respectively.

	p $[GeV/c]$	$\sqrt{s} - M_n$ $[MeV/c^2]$	$M_\Delta(p)$ $[MeV/c^2]$	$\Gamma_\Delta(p)$ $[MeV/c^2]$	$M_\Delta(A)$ $[MeV/c^2]$	$\Gamma_\Delta(A)$ $[MeV/c^2]$	Ref.
1	1.67	1375	1210	89			[3]
2	1.67	1375	1214 ± 0.5	98.0 ± 2.1	1216 ± 0.6	108.0 ± 2.4	[3]
3	2.15	1543	1216	102.5			
4	2.15	1543	1222 ± 4	99 ± 8	1217 ± 5	105 ± 11	
5	1.14	1362	1212 ± 8	72 ± 13			[9]
6	2.80	1763	1220 ± 2	77 ± 2			[10]
7	6.00	2688	1226 ± 6	126 ± 6			[11]

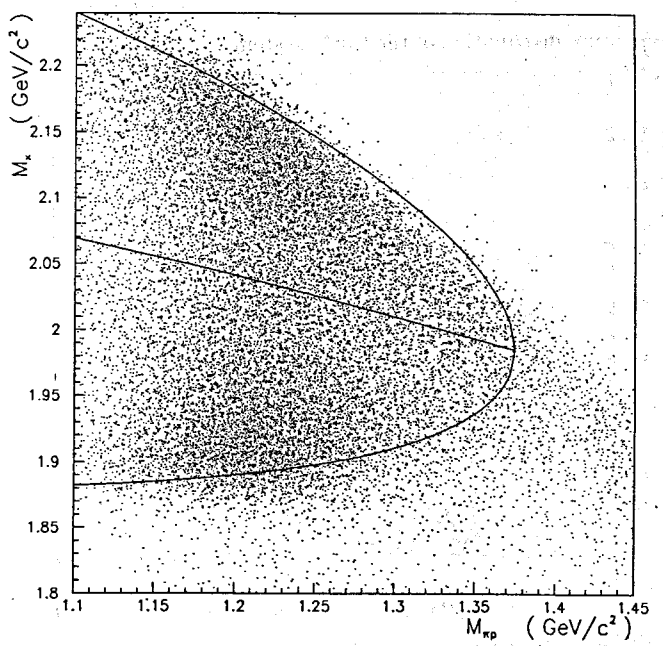

Fig. 1 Scatter plot of the invariant masses: M_X versus $M_{p\pi}$ for the reaction $dp \rightarrow p\pi^+X$.

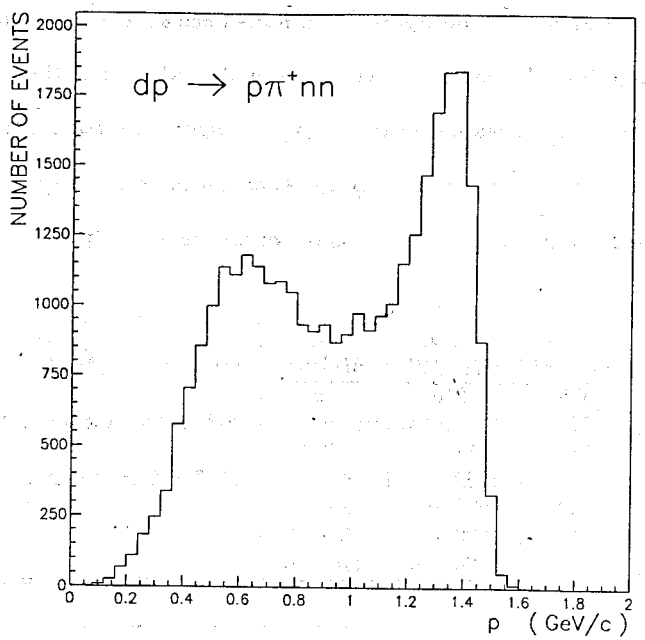

Fig. 2 Momentum distribution of the $(p\pi^+)$ system from the reaction $dp \to p\pi^+ X$.

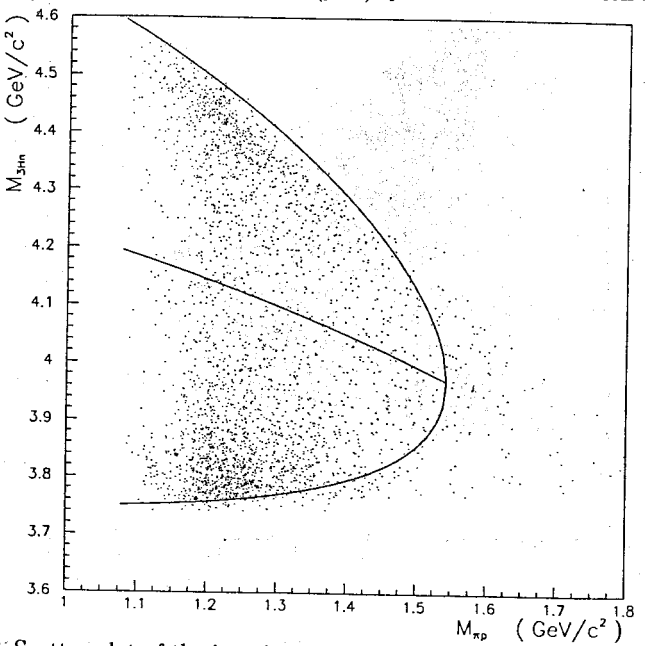

Fig. 3 Scatter plot of the invariant masses: $M(^3H_s n)$ versus $M(p\pi^+)$ for the reaction $^4Hep \to {}^3H_s p n \pi^+$.

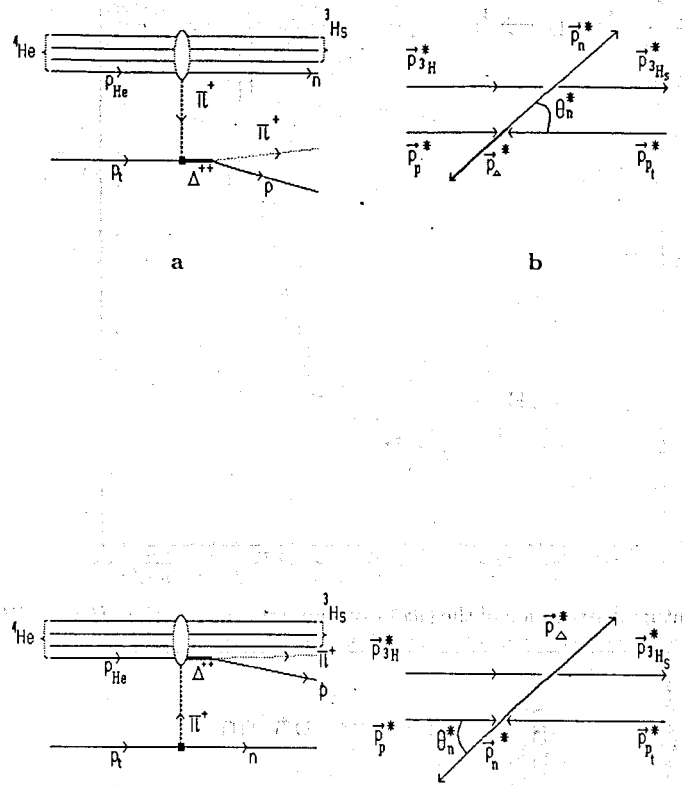

Fig. 4 Diagrams illustrating the $p_{^4He}p_t \to \Delta^{++}n$, $^3H_{^4He} \to {}^3H_s$ reaction kinematics:

a,c) one-pion exchange,

b,d) momentum diagrams in the reaction CMS.

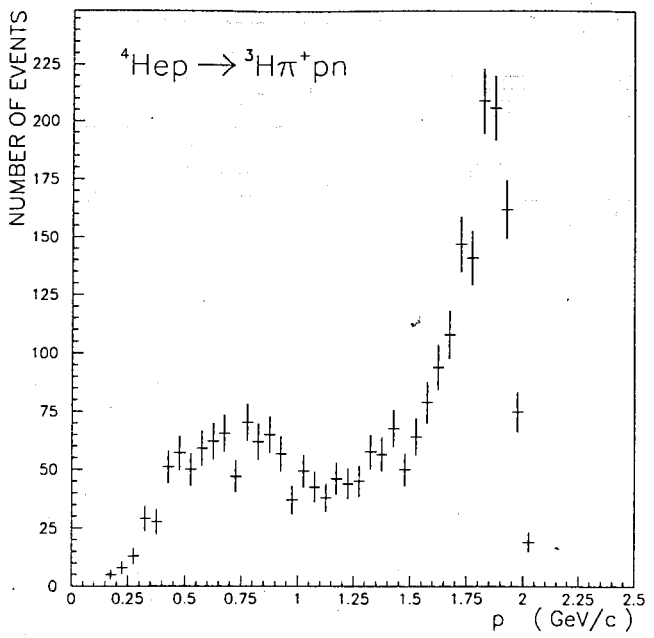

Fig. 5 Momentum distribution of the $(p\pi^+)$ system from the reaction $^4Hep \rightarrow {}^3H_s pn\pi^+$.

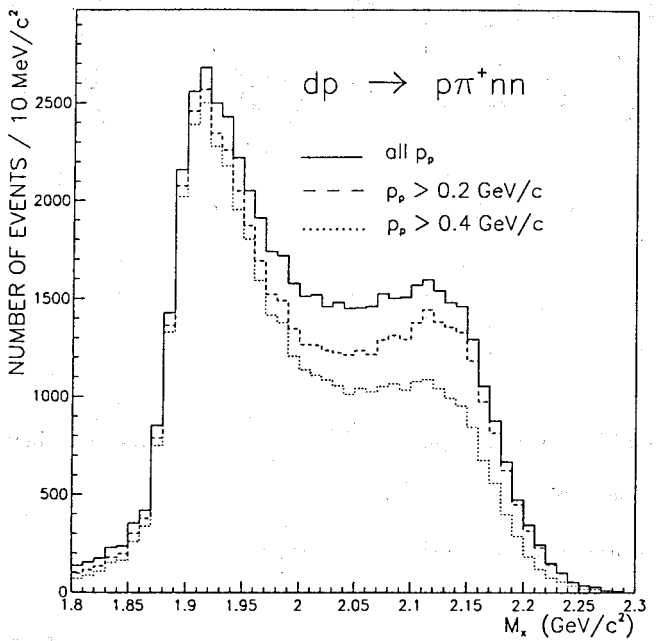

Fig. 6 Missing mass distribution of the (nn) system from the reaction $dp \rightarrow p\pi^+X$.

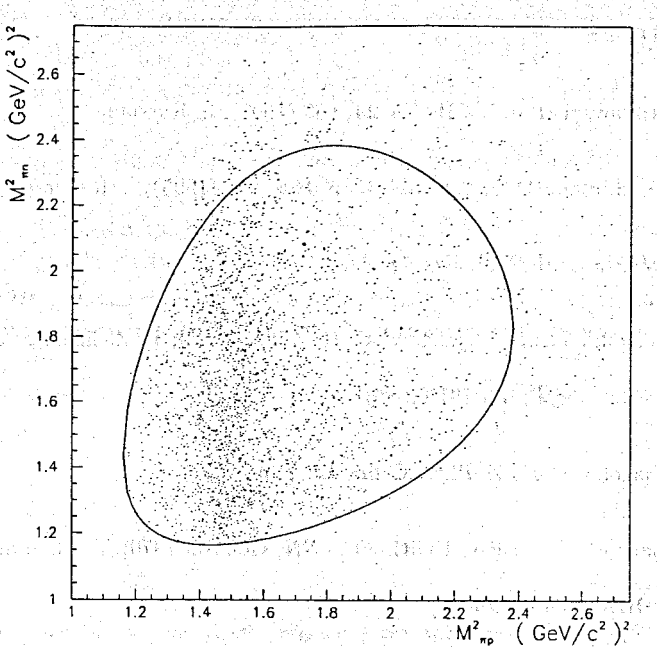

Fig. 7 Dalitz plot: $M^2(n\pi^+)$ versus $M^2(p\pi^+)$ for the reaction $^4Hep \rightarrow {}^3H_s pn\pi^+$.

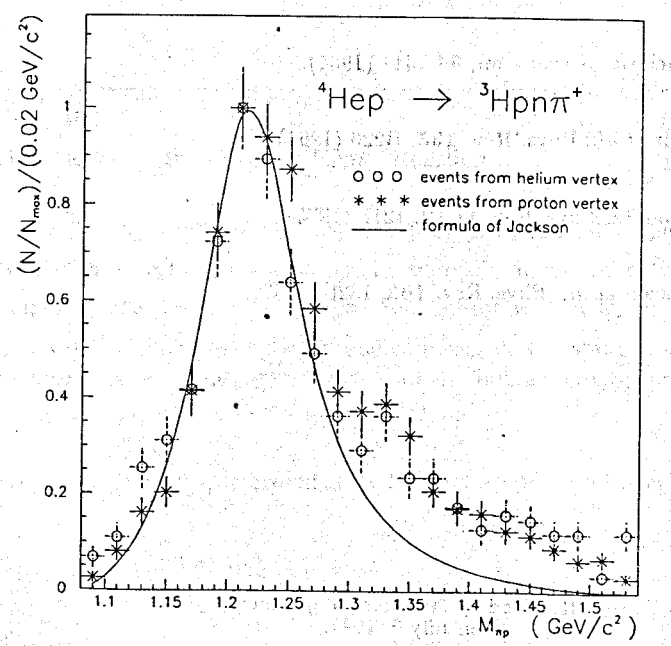

Fig. 8 Invariant mass distribution of the $(p\pi^+)$ system from the reaction $^4Hep \rightarrow {}^3H_s pn\pi^+$.

References

[1] E.A. Strokovski *et al.*, ECHAYA **24**, 603 (1993), in Russian.

[2] K.N. Mukhin and O.O. Pataraki, UFN **165**, 841 (1995), in Russian.

[3] J. Hlaváčová *et al.*, Yad. Fyz. **60**, 464 (1997).

[4] V.V. Glagolev *et al.*, Phys. Rev. **C 18**, 1382 (1978); P. Zielinski *et al.*, Yad. Fiz.(J. Nucl. Phys.) **43**, 791 (1986).

[5] V.V. Glagolev *et al.*, Z. Phys. **C 60**, 421 (1993).

[6] O. Benary *et al.*, CERN, UCRL-20000NN, Geneva, 1970; V. Flaminio *et al.*, CERN, HERA 84-01, 1984.

[7] D.V. Bugg *et al.*, Phys. Rev. **133**, B 1017 (1964).

[8] J.D. Jackson, Nuovo Cim. **34** 1644 (1964).

[9] E. Boldt *et al.*, Phys. Rev. **133**, B220 (1964).

[10] J.D. Mountz, Phys. Rev. **D 12**, 1211 (1975).

[11] T.C. Bacon *et al.*, Phys. Rev. **162**, 1320 (1967).

Received by Publishing Department
on July 9, 1997.